Research Square

Preprints are preliminary reports that have not undergone peer review.
They should not be considered conclusive, used to inform clinical practice,
or referenced by the media as validated information.

Power-Aware and Spectral-Efficiency-Aware Graph-Based Bandwidth Allocation with Alternating Power Control for Multi-UAV 6G Networks

K ollimarla Srinivasa Rao

srinivas.kollimarla.ece@jntua.ac.in

Jawaharlal Nehru Technological University Anantapur

Dr. S. Kannappan

Siddharth Institute of Engineering & Technology, Puttur

Gunturu Jyothi

Jawaharlal Nehru Technological University Anantapur

Research Article

Keywords:

Posted Date: November 19th, 2026

DOI: https://doi.org/10.21203/rs.3.rs-11387657/v1

License: This work is licensed under a Creative Commons Attribution 4.0 International License.
Read Full License

Additional Declarations: No competing interests reported.

Power-Aware and Spectral-Efficiency-Aware Graph-Based Bandwidth Allocation with Alternating Power Control for Multi-UAV 6G Networks

Kollimarla Srinivasa Rao[1*], S. Kannappan[2] and Gunturu Jyothi[1]

[1]Department of Electronics and Communication Engineering, JNTUA College of Engineering, Ananthapuramu, Andhra Pradesh, India.
[2]Department of Electronics and Communication Engineering, Siddarth Institute of Engineering & Technology, Puttur, Andhra Pradesh, India.

*Corresponding author(s). E-mail(s): srinivas.kollimarla.ece@jntua.ac.in;

Abstract

Graph-based bandwidth allocation followed by M-matrix power control is an efficient two-stage design for multi-UAV 6G networks. Its graph reformulation, however, maximizes the total allocated bandwidth rather than the data rate, and it allocates bandwidth with every UAV at maximum power, where interference is highest. We propose three changes. A spectral-efficiency-aware (SE-aware) allocation restores the data-rate objective and is solved exactly as a linear program (LP). A power-aware refinement then searches the UAV power levels, scoring every candidate by that LP while each link keeps at least the worst-link rate of the base design. Finally, an alternating bandwidth–power stage lowers transmit power at unchanged quality-of-service targets. We prove that the first stage is never worse than the base allocation, that the refinement never lowers the data rate, and that the alternating stage never increases power. Over 200 paired Monte Carlo trials per configuration with 3–10 UAVs, the proposed scheme raises the sum data rate by 21–231% and the energy efficiency by 6–95% over the base scheme under line-of-sight conditions (Holm-corrected Wilcoxon $\boldsymbol{p < 0.01}$), and by up to 305% and 111% under mixed line-of-sight/non-line-of-sight conditions. For 3–5 UAVs it attains 87–96% of a near-optimal joint benchmark, against 34–46% for the base scheme. The costs are a lower Jain fairness index, which a tunable rate floor partly restores, and a runtime of 0.3–2.5 s per network.

Keywords: UAV networks, 6G, bandwidth allocation, power control, linear programming, energy efficiency

1 Introduction

Unmanned aerial vehicles (UAVs) act as agile aerial base stations and relays in 6G networks. Their mobility and the high probability of line-of-sight (LoS) links make them attractive for coverage in hard-to-reach areas, disaster recovery, traffic monitoring and mobile edge computing [1–3]. These same properties create new resource-management problems. Strong LoS links mean that UAVs interfere with each other over long distances, and limited on-board energy means that transmit power must be kept low [4]. Bandwidth allocation and power control are therefore tightly coupled, and allocating one without regard to the other wastes spectrum or energy.

Alnakhli et al. [5] proposed an efficient two-stage design for this problem. Stage 1 represents UAV links as a link graph and groups mutually compatible links into maximal independent sets (MISs) that can reuse the same band. It then assigns bandwidth to each MIS by sequential quadratic programming (SQP) with all UAVs at maximum transmit power. Stage 2 minimizes transmit power with M-matrix theory, subject to SINR targets derived from the allocated bandwidths. The scheme clearly outperformed MASPECT [6], a linear-optimization benchmark [7] and random selection, and a recent extension by the same group handles correlated data with a linear bandwidth model and an augmented-Lagrangian power stage [8].

Two limitations remain in the two-stage design, and they are the starting point of this paper. First, its stated goal is to maximize the network data rate, the sum over links of bandwidth times spectral efficiency (Eq. (6) of [5]). The graph reformulation (Eq. (11) of [5]), however, maximizes the sum of allocated bandwidths only, so a megahertz given to a weak link counts as much as one given to a strong link. Second, bandwidth is chosen with all UAVs at maximum power. In the model of [5] every active UAV interferes with every receiver, so maximum power is the worst case for interference, and power is reduced only afterwards to meet rate targets that were themselves fixed under full interference. Neither limitation requires a new system model to fix: both can be removed inside the same graph formulation, which keeps the comparison with [5] direct and fair.

This paper keeps the system model, the MIS structure and the constraints of [5] unchanged and makes three targeted changes, summarized as contributions.

1. **SE-aware graph bandwidth allocation.** We show that the base reformulation omits spectral efficiency from its objective, restore the data-rate objective under the same MIS and fairness constraints, and prove that the resulting problem is a linear program (LP) solved to global optimality.
2. **Power-aware refinement.** A multi-start coordinate search over discrete UAV power levels scores each candidate by the exact SE-aware LP with a per-link rate floor. We prove that it never lowers the data rate and that every link keeps the floor.
3. **Alternating bandwidth–power optimization.** A block-coordinate stage alternates between re-allocating bandwidth at fixed power and minimum-power control at fixed bandwidth. We prove that total power is non-increasing and that every quality-of-service (QoS) target stays met.
4. **Rigorous evaluation.** We use 200 paired Monte Carlo trials per configuration, 95% confidence intervals and Wilcoxon signed-rank tests with Holm correction. The study includes a component ablation, an optimality-gap analysis, 3–10 UAVs, shadowed and mixed LoS/NLoS channels, measured runtime, and QoS and fairness-floor sweeps.

Section 2 reviews related work and Section 3 presents the system model. Section 4 describes the proposed method, Section 5 the simulation setup and Section 6 the results. Section 7 discusses limitations and Section 8 concludes.

2 Related Work

UAV resource allocation.

Early studies established the opportunities and challenges of UAV-assisted wireless networks [1, 2]. For multi-UAV systems, Wu et al. [9] jointly optimized user scheduling, UAV trajectories and transmit power by block-coordinate descent and successive convex approximation. Fu et al. [10] combined a 3D channel model with binary exponential power control for 5G IoT networks. Wang et al. [11] proposed iterative channel allocation and power control to mitigate radar interference in UAV formations. Lee et al. [12] used hierarchical multi-agent Q-learning for frequency reuse and power control. Zhang et al. [13] formulated dynamic bandwidth allocation as many-to-many matching, and Shah and Karabulut [14] applied metaheuristics to drone communication. These works change the solution technique or the network setting; none revisits the objective of the graph-based formulation of [5] or lets transmit power shape its bandwidth allocation.

Graph-based spectrum sharing.

Conflict graphs, whose independent sets are the sets of links that may transmit together, are a

Table 1 Comparison with closely related multi-UAV resource-allocation works

Work	Spectrum	Power	Method
[9]	scheduling	✓	BCD + SCA
[10]	–	✓	exponential power control
[11]	✓	✓	iterative allocation
[12]	✓	✓	multi-agent Q-learning
[13]	✓	–	matching theory
[5]	✓	✓	graph SQP + M-matrix
[8]	✓	✓	linear model, augmented Lagrangian
This work	✓	✓	SE-aware LP, power-aware search, alternating LPs

standard tool for modelling interference in multi-hop and ad hoc networks [15]. Rates obtained by sharing time or bandwidth among independent sets can be optimized by linear programming over those sets [15]. MASPECT [6] and the device-to-device scheme of [7] apply the same graph view to spectrum packing, and [5] carries it to multi-UAV 6G networks. Our Stage 1 stays within this framework and changes only the weights of the independent sets.

Power control and joint optimization.

For fixed SINR targets, minimum-power control has a unique solution whenever the targets are feasible, and it can be found by linear algebra or by distributed iterations [16, 17]; the M-matrix method of [5] is an instance of this theory. Jointly maximizing the sum rate over powers and spectrum, by contrast, is NP-hard in general [18]. Practical designs therefore decompose the problem into blocks and optimize them alternately, with convergence guarantees from block-coordinate descent theory [9, 19]. We follow this route: every block we solve is an exact LP, and only the outer search over discrete power levels is heuristic.

Table 1 positions this paper against the closest works.

3 System Model and Problem Formulation

We adopt the system model of [5] unchanged, so that every difference in results comes from the algorithm.

Network and channel.

M UAVs hover with a vertical separation of 50 m, and their horizontal separations are uniform in $[1, 100]$ m. The distance between UAVs i and j is

$$d_{ij} = \sqrt{\left(d_{ij}^{H}\right)^2 + \left(d_{ij}^{V}\right)^2}, \tag{1}$$

and the air-to-air LoS path loss [20] is

$$PL_{ij}\,[\mathrm{dB}] = PL(d_0) + 10\,\alpha \log_{10}\left(\frac{d_{ij}}{d_0}\right), \tag{2}$$

with $PL(d_0) = 46.4\,\mathrm{dB}$, $d_0 = 1\,\mathrm{m}$ and $\alpha = 2.03$, giving the channel gain $h_{ij} = 10^{-PL_{ij}/10}$. Section 6.5 adds log-normal shadowing and mixed LoS/NLoS links, a simplified form of the probabilistic LoS models used for low-altitude platforms [21].

Topology.

A random connection graph $G(V, E)$ links a fraction ρ (the network density) of all UAV pairs. Each edge $k = (i, j)$ is a bidirectional link. In the link graph $\hat{G}$, two links conflict if they share a UAV. Each MIS q of $\hat{G}$ is a set of links that can reuse the same band, and $s_{qk} = 1$ if link k belongs to MIS q. Fig. 1 illustrates the model.

Rate.

With transmit powers $\mathbf{P}_t$, the SINR from UAV i to UAV j is

$$\mathrm{SINR}_{ij} = \frac{P_{t,i}\,h_{ij}}{\sum_{v \neq i,j} P_{t,v}\,h_{vj} + \rho_0}, \tag{3}$$

where the sum runs over active UAVs and $\rho_0 = -147 + 10\log_{10} B_{\mathrm{tot}} + 10\,\mathrm{dBm}$ is the noise power. The spectral efficiency of link k is $R_k(\mathbf{P}_t) = \log_2(1+\mathrm{SINR}_{ij}) + \log_2(1+\mathrm{SINR}_{ji})$, its bandwidth is $B_k = \sum_q s_{qk} X_q$, and the network data rate is $\sum_k B_k R_k$.

Base problem.

The goal of [5] is to maximize $\sum_k B_k R_k$ subject to $\sum_q X_q = B_{\mathrm{tot}}$ and $P_{t,i} \le P_{t,\max}$. Stage 1 fixes $\mathbf{P}_t = P_{t,\max}$ and, with traffic shares $g_k =$

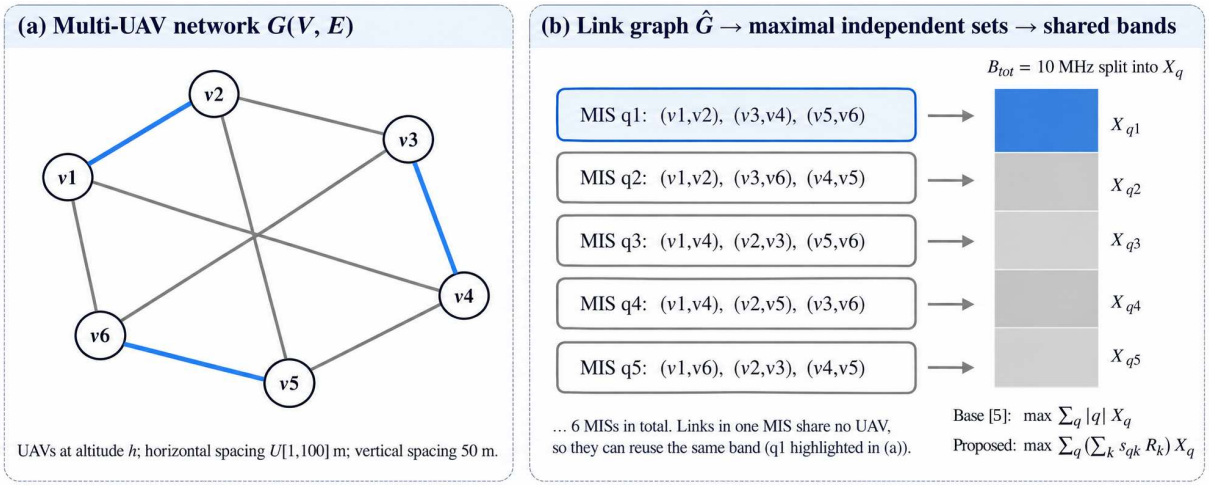


Fig. 1 Network model. (a) Example network $G(V, E)$ with six UAVs; the links of one maximal independent set (q_1) are highlighted. (b) The MISs of the link graph $\hat{G}$; each MIS q receives a band X_q, and the base and SE-aware schemes differ in how the bands are weighted.

$R_k / \sum_l R_l$, solves

$$\max_{\mathbf{X}\geq 0} \sum_k \sum_q s_{qk} X_q$$
$$\text{s.t.} \sum_q X_q = B_{\text{tot}}, \quad \sum_q s_{qk} X_q \geq B_{\text{tot}}\, g_k \quad \forall k. \tag{4}$$

The objective of (4) counts allocated bandwidth, not data rate: R_k no longer appears. Stage 2 then minimizes $\sum_i P_{t,i}$ subject to rate targets c_k on every link, using $\varphi_k = 2^{c_k/B_k} - 1$ as the SINR target.

Table 2 Main notation

Symbol	Meaning
M, K, Q	numbers of UAVs, links and MISs
s_{qk}	1 if link k belongs to MIS q
X_q, B_k	bandwidth of MIS q; of link k
$\mathbf{P}_t$, $P_{t,\max}$	UAV transmit powers; power limit
$R_k(\mathbf{P}_t)$	spectral efficiency of link k (both directions)
g_k, τ	traffic share of link k; fairness scaling
$r_{\min}$, κ	per-link rate floor; floor factor
c_{kd}, β	rate target of direction d of link k; QoS factor
$F(\mathbf{P}_t)$	optimal data rate of (P3) at powers $\mathbf{P}_t$

4 Proposed Method

The proposed scheme keeps the two-stage structure of [5] and adds three components: a new Stage-1 objective, a power-aware refinement (Stage 1b) and an alternating stage after power control (Stage 3). Fig. 2 shows the complete processing chain.

Design rationale.

The joint problem of choosing powers and bandwidths to maximize the sum rate is NP-hard in general [18], so an exact joint solution is out of reach. Our design separates what can be solved exactly from what cannot. For any fixed power vector, the bandwidth problem over the MISs is an LP, which we always solve to global optimality; for fixed bandwidths, minimum-power control is also an LP. The only heuristic part is the outer search over a small set of discrete power levels in Stage 1b, and every candidate it visits is scored by the exact LP. Each stage keeps a feasible solution and only accepts improvements, which yields the monotonicity guarantees of Propositions 1–3. Table 2 lists the main notation.

4.1 SE-aware bandwidth allocation (Stage 1)

At fixed powers each R_k is a constant, so the data-rate objective is linear in the MIS bandwidths X_q. Keeping every constraint of the base problem, we

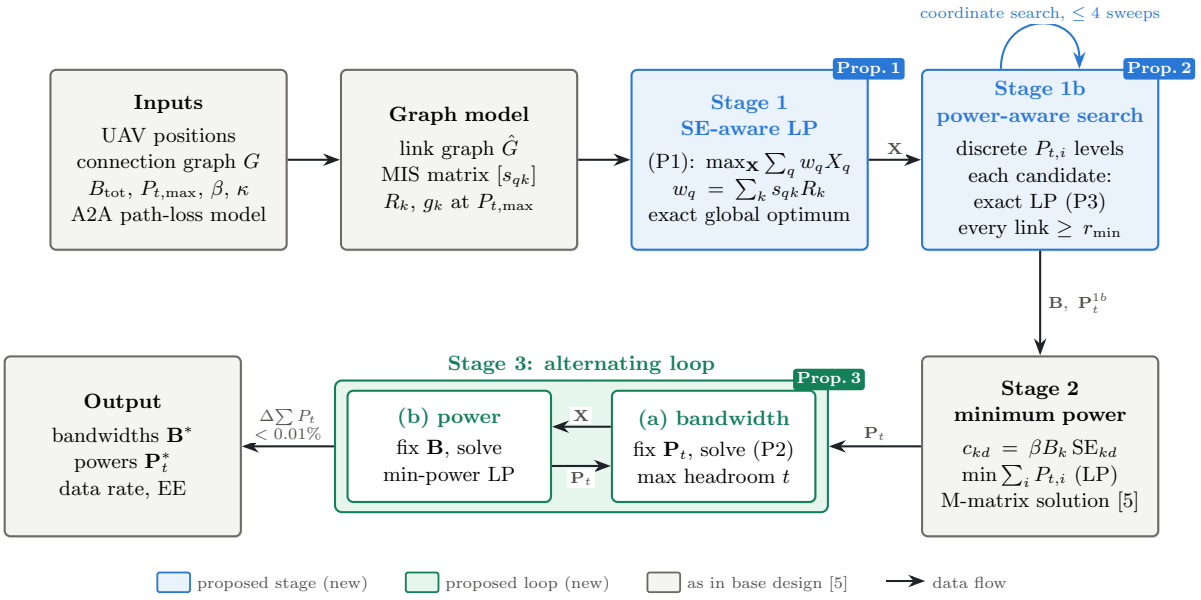


Fig. 2 Block diagram of the proposed scheme. Stages 1 and 1b (blue) and Stage 3 (green) are the new components; Stage 2 is the minimum-power control of [5].

solve

$$\text{(P1)} \quad \max_{\mathbf{X}\geq 0} \sum_q w_q X_q, \qquad w_q = \sum_k s_{qk} R_k$$
$$\text{s.t.} \sum_q X_q = B_{\text{tot}}, \tag{5}$$
$$\sum_q s_{qk} X_q \geq \tau \, B_{\text{tot}} \, g_k \quad \forall k.$$

Here $\tau \leq 1$ is the largest value for which the fairness constraint of (4) is feasible ($\tau = 1$ whenever the base constraint is feasible); the same τ is used for the base scheme in every comparison.

Proposition 1. *(P1) is a linear program, so any LP solver returns its global optimum. Its feasible set equals that of the base problem; hence, at maximum power, the data rate of the SE-aware allocation is never lower than that of the base allocation.*

Proof. The objective is a weighted sum of X_q with constant weights w_q, and all constraints are linear in $\mathbf{X}$. Only the objective changed, so the feasible sets coincide and the base allocation is feasible for (P1). Global optimality of (P1) over that set gives the inequality. □

The base objective is the special case $w_q = |q|$, the number of links in MIS q. The base design therefore favours large MISs regardless of link quality, whereas (P1) favours MISs whose links carry high spectral efficiency.

Illustrative example.

Consider $B_{\text{tot}} = 10\,\text{MHz}$, an MIS q_1 containing two weak links with $R_k = 1\,\text{bit/s/Hz}$ each, and an MIS q_2 containing one strong link with $R_k = 6\,\text{bit/s/Hz}$, where each MIS must receive at least 1 MHz. The base objective weights the MISs by their sizes, $w_1 = 2$ and $w_2 = 1$, so it gives $X_1 = 9\,\text{MHz}$ and $X_2 = 1\,\text{MHz}$, for a data rate of $9 \cdot 2 + 1 \cdot 6 = 24\,\text{Mbps}$. The SE-aware objective uses $w_1 = 2$ and $w_2 = 6$, so it gives $X_1 = 1\,\text{MHz}$ and $X_2 = 9\,\text{MHz}$, for $1 \cdot 2 + 9 \cdot 6 = 56\,\text{Mbps}$. Both allocations satisfy exactly the same constraints; only the objective differs.

4.2 Power-aware refinement (Stage 1b)

Because every active UAV interferes with every receiver in (3), lowering the power of a strong interferer can raise the data rate of many other links. For a power vector $\mathbf{P}_t$, let $F(\mathbf{P}_t)$ be the

optimal value of

$$\begin{aligned}(\text{P3}) \quad \max_{\mathbf{X}\geq 0} \; & \sum_q X_q \sum_k s_{qk} R_k(\mathbf{P}_t) \\ \text{s.t. the constraints of (P1)}, \\ & B_k\, R_k(\mathbf{P}_t) \geq r_{\min} \quad \forall k,\end{aligned} \tag{6}$$

where $B_k = \sum_q s_{qk} X_q$, with $F = -\infty$ when (P3) is infeasible. The rate floor $r_{\min} = \kappa \min_k r_k^{\text{base}}$ is κ times the worst-link rate of the base allocation at maximum power, so no link is left behind; $\kappa = 1$ by default. For fixed $\mathbf{P}_t$, (P3) is again an LP. Searching powers directly would require solving a non-convex problem [18]; instead, Stage 1b treats F as a black box that is cheap and exact to evaluate.

Stage 1b maximizes F over the power levels $P_{t,i} \in P_{t,\max} \cdot \{1, 0.5, 0.25, 0.1, 0.05, 0.02, 0.01, 0.003, 0.001\}$. It starts from $P_{t,\max}$ and 20 random power vectors, keeps the three best, and improves each by coordinate search: one UAV's power changes at a time, and a change is kept only if F increases. At most four sweeps are made, and the best power vector, with its LP allocation, is passed to Stage 2.

Proposition 2. *If (P3) is feasible at $\mathbf{P}_t = P_{t,\max}$, Stage 1b returns a data rate no lower than that of (P1) with the floor $r_{\min}$, and every link meets $r_{\min}$.*

Proof. $P_{t,\max}$ is a starting point and is kept unless a candidate with a higher F is found, and the coordinate search accepts only strict increases of F. Every accepted candidate has finite F, so its LP allocation satisfies the floor constraint of (6). □

If no candidate is feasible, the scheme falls back to the (P1) solution at maximum power; this never happened in our experiments (feasibility was 100% in all configurations).

4.3 Minimum-power control (Stage 2)

For direction d of link k, the rate target is $c_{kd} = \beta B_k \log_2\big(1 + \text{SINR}_{kd}(\mathbf{P}_t^{1b})\big)$, where $\mathbf{P}_t^{1b}$ is the Stage-1b power vector and $\beta \in (0, 1]$ is the QoS factor, giving the SINR target $\varphi_{kd} = 2^{c_{kd}/B_k} - 1$. With φ fixed, each constraint is linear in $\mathbf{P}_t$:

$$\begin{aligned} & P_{t,t}\, h_{tr} \;\geq\; \varphi_{kd}\Big(\sum_{v\neq t,r} P_{t,v}\, h_{vr} + \rho_0\Big), \\ & 0 \leq P_{t,i} \leq P_{t,\max}, \end{aligned} \tag{7}$$

Minimizing $\sum_i P_{t,i}$ under (7) is an LP. By standard power-control theory, whenever the targets are feasible the minimum-power vector is unique and componentwise smallest [16, 17]. When each UAV serves a single link, its solution is the M-matrix (Sherman–Morrison) solution of [5]; when a UAV serves several links, the LP keeps every link's constraint. Because $\mathbf{P}_t^{1b}$ satisfies all targets ($\beta \leq 1$), the LP is always feasible.

4.4 Alternating bandwidth–power optimization (Stage 3)

After Stage 2, a different bandwidth split may meet the same targets with less power. Stage 3 alternates two exact LPs with c_{kd} held fixed. In the bandwidth step, for fixed $\mathbf{P}_t$ and with $\text{SE}_{kd}(\mathbf{P}_t) = \log_2(1 + \text{SINR}_{kd}(\mathbf{P}_t))$, it maximizes the common headroom t:

$$\begin{aligned}(\text{P2}) \quad \max_{\mathbf{X}\geq 0,\, t} \; & t \\ \text{s.t.} \; & \sum_q X_q = B_{\text{tot}}, \\ & B_k\, \text{SE}_{kd}(\mathbf{P}_t) \geq t\, c_{kd} \quad \forall k, d,\end{aligned} \tag{8}$$

In the power step, it solves the minimum-power LP for the new bandwidths. The loop stops when total power falls by less than 0.01% or after 20 iterations.

Proposition 3. *Total transmit power is non-increasing over the iterations of Stage 3, and every rate target c_{kd} is met at every iteration.*

Proof. At iteration n the pair $(\mathbf{X}^{(n)}, \mathbf{P}_t^{(n)})$ meets all targets, so $\mathbf{X}^{(n)}$ is feasible for (P2) with $t \geq 1$. The optimum $\mathbf{X}^{(n+1)}$ therefore has $t \geq 1$, so $\mathbf{P}_t^{(n)}$ still meets every target under $\mathbf{X}^{(n+1)}$. Hence $\mathbf{P}_t^{(n)}$ is feasible for the power step, whose optimum satisfies $\sum_i P_{t,i}^{(n+1)} \leq \sum_i P_{t,i}^{(n)}$. A non-increasing sequence bounded below by zero converges. This is the standard monotonicity argument of block-coordinate descent [19]. □

Table 3 Simulation parameters (as in [5] unless marked "new")

Parameter	Value
α; d_0; $PL(d_0)$	2.03; 1 m; 46.4 dB
Vert. / horiz. separation	50 m / uniform $[1, 100]$ m
B_{tot}; $P_{t,\max}$	10 MHz; 1 W
Noise power ρ_0	$-147 + 10\log_{10} B_{\text{tot}} + 10$ dBm
Number of UAVs	3–8; 9 and 10 (scalability, new)
Network density ρ	0.5, 0.8, 1.0
QoS factor β	0.8; sweep 0.5–0.9 (new)
Rate-floor factor κ (new)	1; sweep 0–2
Stage-1b power levels (new)	$P_{t,\max} \times \{1, .5, .25, .1, .05, .02, .01, .003, .001\}$
Stage-1b search (new)	21 starts; best 3 refined; ≤ 4 sweeps
Shadowing (new)	log-normal, $\sigma = 4$ dB
Mixed LoS/NLoS (new)	$P_{\text{LoS}} = 0.7$, NLoS exponent 3.0, $\sigma = 6$ dB
Alternating stage	≤ 20 iterations; stop at $< 0.01\%$ decrease
Monte Carlo trials	200 per configuration (50 for $N \geq 9$ and sweeps)

4.5 Algorithm and complexity

Algorithm 1 summarizes the scheme. Each LP has $Q+1$ or M variables and at most $3K$ constraints, where Q is the number of MISs and K the number of links; the HiGHS solver [22] solves each in a few milliseconds. Stage 1b solves one LP per candidate (178–543 LPs on average for 3–8 UAVs), so it dominates the runtime (Section 6.6). MIS enumeration grows quickly with network size and is shared by all schemes.

5 Simulation Setup

All schemes run on identical random networks in each trial (a paired design), so the differences reflect the algorithms alone. The simulator is written in Python with NumPy, SciPy (HiGHS LP solver) and NetworkX, and runtimes were measured on a 2-core Intel Xeon 2.10 GHz cloud instance. Table 3 lists the parameters.

Schemes compared.

Base SQP [5]: problem (4) followed by minimum-power control; we solve (4) exactly as an LP, which is the best result SQP can reach, so the comparison favours the base scheme. *Base SLSQP, random start*: (4) solved by SLSQP from a random starting point, as in Algorithm 1 of [5]. *Equal MIS bandwidth*: B_{tot} split equally over all MISs, then power control. *Random selection*: random bandwidths and powers, as in [5]. *Proposed (full)*: Stages 1, 1b, 2 and 3. *Ablations*: SE-aware only (Stages 1–2), SE-aware + alternating (Stages 1–3 without 1b), SE-aware + power-aware (Stages 1, 1b and 2), and the base and proposed schemes without power control. MASPECT [6] is not re-implemented, because [5] does not give enough detail to reproduce it faithfully; it was outperformed by the base scheme in [5].

Near-optimal benchmark.

For 3–5 UAVs (30 networks each, $\rho = 0.8$), we approximate the best joint solution of (P3) over continuous powers by the best of 300 random power vectors and $P_{t,\max}$, each scored by the exact LP, polished by 400 Nelder–Mead iterations. The better of this benchmark and Stage 1b is the reference value.

Metrics and statistics.

We report the sum data rate $\sum_k B_k R_k$ (Mbps), the energy efficiency (EE), defined as data rate divided by total transmit power (Gbit/J), the minimum link rate, the runtime per network, and Jain's fairness index [23]

$$J = \frac{\left(\sum_{k=1}^{K} r_k\right)^2}{K \sum_{k=1}^{K} r_k^2}, \tag{9}$$

where $r_k = B_k R_k$ is the data rate of link k. J ranges from $1/K$, when one link receives all the rate, to 1, when all links receive equal rates; it measures fairness, not gain. For every metric we give the mean and its 95% confidence interval $(1.96\, s/\sqrt{n})$. The proposed scheme is compared with each baseline by a one-sided paired Wilcoxon signed-rank test [24] with Holm correction across baselines [25].

6 Results and Discussion

The proposed scheme improves both data rate and EE over the base scheme in all 18 main configurations. The data-rate gain is 21–231%, the EE gain is 6–95%, and every gain is significant at $p_{\text{Holm}} < 0.01$.

Algorithm 1 Proposed power-aware, SE-aware allocation with alternating power control

Require: positions, connection graph G, B_{tot}, $P_{t,\max}$, β, κ

Build the link graph $\hat{G}$ and enumerate its MISs $[s_{qk}]$
Compute R_k, g_k at $P_{t,\max}$; find τ; solve (4) once to obtain $r_{\min}$
Stage 1b: evaluate F by (P3) at $P_{t,\max}$ and 20 random power vectors
for each of the three best candidates **do**
    repeat ▷ at most four sweeps
        for each active UAV i and power level ℓ **do**
            set $P_{t,i} \leftarrow \ell$; keep the change only if F increases
        end for
    until no change improves F
end for
Keep the best $(\mathbf{P}_t^{1b}, \mathbf{X})$; set $c_{kd} = \beta B_k \log_2(1 + \text{SINR}_{kd}(\mathbf{P}_t^{1b}))$
Stage 2: solve the minimum-power LP for $\mathbf{P}_t$
repeat ▷ Stage 3
    solve (P2) for $\mathbf{X}$ at the current $\mathbf{P}_t$; solve the minimum-power LP for $\mathbf{P}_t$
until $\sum_i P_{t,i}$ decreases by less than 0.01%
return $(\mathbf{B}, \mathbf{P}_t)$

Table 4 Gain of the proposed scheme over Base SQP (%), 200 paired trials

	Data-rate gain (%)			EE gain (%)		
N	ρ=0.5	0.8	1.0	0.5	0.8	1.0
3	139.2	142.4	21.5	30.3	34.2	20.0
4	111.0	106.6	70.1	12.4	5.8	21.3
5	173.2	180.2	177.0	33.8	63.1	83.7
6	167.3	155.3	158.5	45.8	50.0	63.6
7	208.7	225.3	230.9	68.5	87.2	95.1
8	209.4	204.2	201.6	64.5	74.0	77.0

All gains are significant at $p_{\text{Holm}} < 0.001$, except the EE gain at 4 UAVs and $\rho = 0.8$ ($p_{\text{Holm}} = 0.009$).

6.1 Data rate and energy efficiency

Fig. 3 plots the mean data rate and EE, with 95% confidence intervals, against the number of UAVs; Table 4 lists the gains over the base scheme.

The base scheme's data rate falls from about 20 to 15 Mbps as UAVs are added, because full-power transmission makes every new UAV a strong interferer. Network density has a second, smaller effect: denser networks contain more links and more MISs, so both the SE-aware LP and Stage 1b have more allocations to choose from, which is why the EE gains are largest at $\rho = 1.0$ for 5–8 UAVs. For 4–8 UAVs the proposed scheme keeps 37–47 Mbps: Stage 1b lowers the power of UAVs whose interference costs the network more than their own links contribute, and the SE-aware LP routes bandwidth to the links that benefit.

Table 5 Absolute results at $\rho = 0.8$ (mean ± 95% CI)

N	Scheme	Rate (Mbps)	EE (Gbit/J)	Jain	Min. rate (Mbps)
4	Base SQP	19.96±0.58	0.0569±0.0021	0.681	0.995
	Proposed	41.24±1.72	0.0602±0.0026	0.372	1.176
6	Base SQP	17.16±0.41	0.0584±0.0018	0.485	0.129
	Proposed	43.82±1.10	0.0876±0.0020	0.116	0.128
8	Base SQP	15.55±0.34	0.0567±0.0014	0.337	0.035
	Proposed	47.30±0.96	0.0987±0.0020	0.058	0.034
	Equal bw.	12.99±0.10	0.0475±0.0008	0.813	0.212
	Random	4.71±0.08	0.0012±0.0000	0.532	0.009

Jain: Jain's fairness index (9), from $1/K$ (one link takes all) to 1 (equal rates); higher is fairer.

The EE gain is smaller than the data-rate gain, because Stage 1b often keeps a few UAVs at high power to carry most of the traffic; it grows from 6–34% at 3–4 UAVs to 64–95% at 7–8 UAVs.

In every main (LoS) configuration, the worst link of the proposed scheme stays within 4% of the base scheme's worst link (Table 5); the small shortfall comes from the β-scaled targets of Stage 2, which both schemes share.

6.2 How the power-aware stage achieves its gain

To see what Stage 1b actually does, we recorded the power levels it selects in 60 networks for each of $N = 4$, 6 and 8 at $\rho = 0.8$. Table 6 summarizes

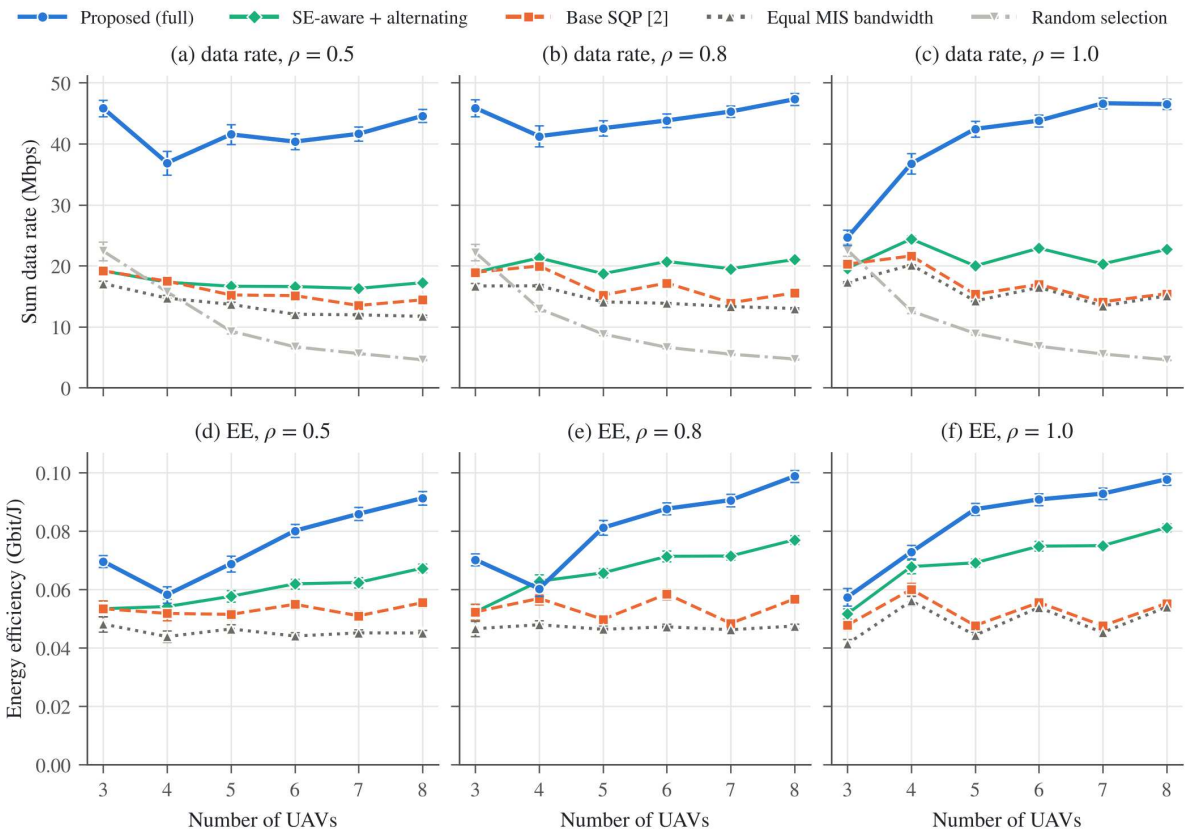


Fig. 3 Sum data rate (a)–(c) and energy efficiency (d)–(f) versus the number of UAVs for three network densities (mean ± 95% CI, 200 paired trials). Random selection is omitted from (d)–(f) because its EE (≤ 0.018 Gbit/J) would compress the other curves.

Table 6 Power levels selected by Stage 1b ($\rho = 0.8$, 60 networks per size)

N	Share of UAVs at $\leq 0.1\,P_{t,\max}$	Share of UAVs at $\geq 0.5\,P_{t,\max}$	Rate share of top 25% links
4	39%	55%	75%
6	62%	31%	94%
8	75%	22%	97%

the result. As the network grows, Stage 1b turns an increasing share of UAVs down to at most 10% of $P_{t,\max}$: 39% of them at $N = 4$ and 75% at $N = 8$. The remaining UAVs stay at high power and carry most of the traffic; at $N = 8$, the strongest quarter of the links carries 97% of the data rate.

This behaviour follows directly from the interference model. In (3) every active UAV adds interference at every receiver, so a UAV whose own links are weak can cost the network more rate through interference than it delivers. Lowering its power raises the SINR of all other links, and the SE-aware LP then moves bandwidth to the links that gained the most. The rate floor $r_{\min}$ prevents this from being taken to the extreme: a throttled UAV still delivers at least the worst-link rate of the base scheme. The same mechanism explains both the large data-rate gains, which grow with N because more UAVs means more mutual interference to remove, and the lower Jain index discussed in Section 6.7.

6.3 Ablation study

Table 7 separates the contribution of each component. Stage 1b is the dominant source of gain, the SE-aware objective is the second, and the alternating stage adds a small but significant EE improvement.

Table 7 Ablation at $N = 6$, $\rho = 0.8$ (mean ± 95% CI)

Variant	Rate (Mbps)	EE (Gbit/J)	Jain
Base SQP	17.16 ± 0.41	0.0584 ± 0.0018	0.485
Base SLSQP, rand.	16.37 ± 0.22	0.0558 ± 0.0014	0.700
Equal MIS bw.	13.84 ± 0.15	0.0472 ± 0.0011	0.818
SE-aware only	20.72 ± 0.33	0.0707 ± 0.0019	0.362
SE + alternating	20.70 ± 0.33	0.0713 ± 0.0019	0.361
SE + power-aware	43.86 ± 1.10	0.0872 ± 0.0020	0.116
Proposed (full)	43.82 ± 1.10	0.0876 ± 0.0020	0.116
Base, no PC	20.66 ± 0.51	0.0034 ± 0.0001	0.486
Proposed, no PC	53.84 ± 1.38	0.0327 ± 0.0015	0.113

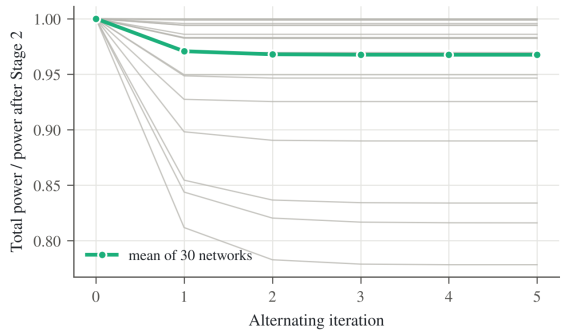


Fig. 4 Total transmit power over the alternating iterations, normalized to its value after Stage 2 ($N = 5$, $\rho = 0.8$; grey: individual networks).

The SE-aware objective raises the data rate and EE by 21% each over the base scheme. Stage 1b more than doubles the data rate again (20.72 to 43.86 Mbps) and adds 23% EE. The alternating stage adds 1.4%, 0.5% and 0.4% EE over SE-aware + power-aware at $N = 4$, 6 and 8 ($p < 0.001$); its effect is small because Stage 1b has already removed most of the excess power. Power control remains essential: without it the proposed scheme's EE falls by 63%. Finally, SLSQP from a random start reaches a lower data rate than the exact solution of the same problem (4) (16.37 versus 17.16 Mbps), so all comparisons use the stronger, exactly solved base.

Fig. 4 shows total power over the alternating iterations for 30 networks with $N = 5$ and $\rho = 0.8$. Every curve is non-increasing, as Proposition 3 requires; the mean reduction is 3.3%, almost all in the first iteration.

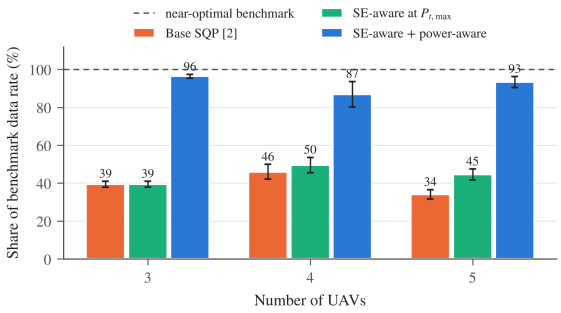


Fig. 5 Data rate of each scheme as a percentage of the near-optimal joint benchmark ($\rho = 0.8$, 30 networks per size, mean ± 95% CI).

6.4 Optimality gap

Fig. 5 compares each scheme's Stage-1 data rate with the near-optimal benchmark. The base scheme and the SE-aware allocation at maximum power reach only 34–46% and 39–50% of the benchmark, because both allocate bandwidth under full interference. With Stage 1b, the proposed scheme reaches 96.4%, 86.9% and 93.3% for 3, 4 and 5 UAVs, with worst cases of 92%, 29% and 70% over the 30 networks. The poor case at $N = 4$ is a network where the coordinate search stopped in a local optimum; more random starts would reduce such cases at a higher runtime.

6.5 Channel robustness and network scale

The gains grow under shadowing and mixed LoS/NLoS conditions and remain large for 9 and 10 UAVs (Table 8).

6.6 Runtime

Table 9 reports the mean runtime per network. The base scheme and the SE-aware + alternating variant take milliseconds. The full scheme takes 0.28–2.5 s, of which Stage 1b accounts for over 95%. This suits UAV networks re-optimized every few seconds, but not per-packet scheduling. Where time is short, the SE-aware + alternating variant still gives 22–48% more EE than the base scheme for 6–8 UAVs at $\rho = 0.8$, in 13–21 ms.

Table 8 Proposed versus Base SQP under other channels ($\rho = 0.8$) and for larger networks ($\rho = 0.5$)

Scenario	UAVs	Data rate (Mbps) base → proposed	Gain	EE (Gbit/J) base → proposed	Gain
LoS + 4 dB shadowing	4	28.21 → 59.17	+109.7%	0.0763 → 0.0965	+26.5%
	6	22.36 → 71.63	+220.3%	0.0800 → 0.1352	+68.9%
	8	20.48 → 84.94	+314.7%	0.0749 → 0.1503	+100.6%
Mixed LoS/NLoS	4	48.72 → 79.23	+62.6%	0.0592 → 0.0895	+51.3%
	6	36.37 → 103.15	+183.6%	0.0635 → 0.1079	+70.0%
	8	32.06 → 129.84	+304.9%	0.0604 → 0.1275	+111.2%
LoS, larger network	9	13.02 → 47.47	+264.7%	0.0518 → 0.0947	+82.9%
	10	14.23 → 49.15	+245.4%	0.0567 → 0.0980	+72.9%

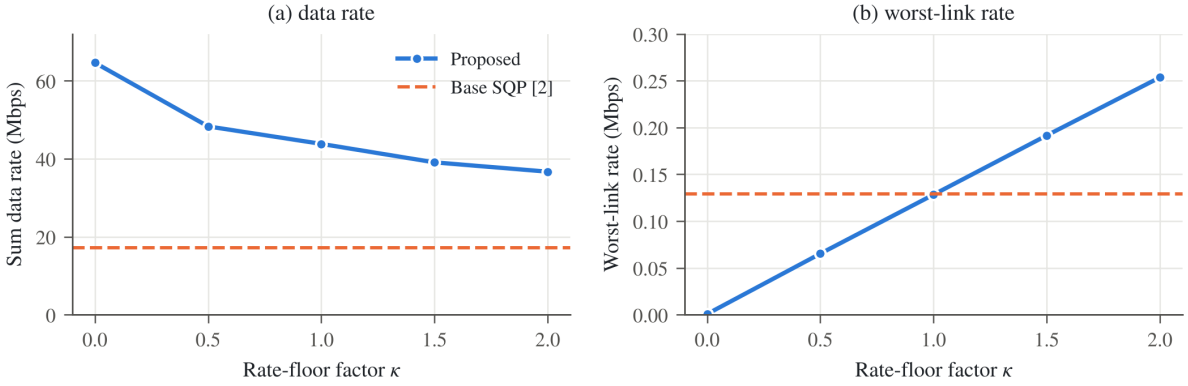


Fig. 6 Effect of the rate-floor factor κ ($N = 6$, $\rho = 0.8$; $\kappa = 1$: 200 trials, others: 50). Dashed: base scheme.

Table 9 Mean runtime per network (ms), excluding MIS enumeration shared by all schemes

N	Base SQP	SE + alternating	Proposed (full)
3	5.0	11.9	282
4	5.1	12.3	344
5	5.2	17.5	602
6	5.5	12.9	740
7	6.0	21.0	1077
8	6.5	15.2	1336
9	6.7	18.4	1671
10	7.5	20.0	2495

Table 10 Effect of the QoS factor β ($N = 6$, $\rho = 0.8$, 50 trials)

	Data rate (Mbps)		EE (Gbit/J)	
β	Base SQP	Proposed	Base SQP	Proposed
0.5	11.20	28.26	0.1518	0.1917
0.6	13.18	33.61	0.1194	0.1534
0.7	15.07	38.87	0.0884	0.1185
0.8	16.90	44.06	0.0588	0.0868
0.9	18.67	49.17	0.0305	0.0581

6.7 QoS factor and fairness floor

The advantage holds for every QoS factor (Table 10). As β rises from 0.5 to 0.9, the data-rate gain over the base scheme stays at 152–163%, and the EE gain grows from 26% to 90%.

Maximizing the sum rate concentrates rate on the strongest links, so the proposed scheme's Jain index is much lower than the base scheme's (0.116 versus 0.485 at $N = 6$, $\rho = 0.8$). The rate-floor factor κ controls this trade-off (Fig. 6). Without a floor ($\kappa = 0$) the data rate reaches 64.6 Mbps but the worst link is almost starved. With $\kappa = 2$, every link receives at least twice the base scheme's worst-link rate (0.254 versus 0.129 Mbps), and the scheme still delivers 2.1 times the base data rate

and 45% more EE. The Jain index, however, stays below the base scheme's for every κ tested (0.102–0.145).

6.8 Comparison with the values reported in [5]

Our implementation of the base scheme gives 20.3 Mbps for three fully connected UAVs, close to the 25.6 Mbps reported in [5]. As UAVs are added, however, [5] reports a steep decline to about 2 Mbps at eight UAVs, whereas our implementation stays near 15 Mbps; the EE values in [5] (about 9 Gbit/J) are also roughly two orders of magnitude above ours. Reference [5] does not specify the minimum rate requirements c_k of its power stage or every detail of how link rates are aggregated, and these choices strongly affect both quantities. We therefore compare all schemes within one implementation on identical networks, and the full code is public so that every number in this paper can be reproduced.

7 Limitations

- **Model scope.** We keep the static model of [5], in which every active UAV interferes regardless of band. Stage 1b exploits this coupling, so its gains would be smaller under a model with orthogonal bands across MISs. Mobility and measured channel traces are not modelled.
- **Fairness.** The sum-rate objective lowers Jain's index substantially. The rate floor protects the worst link but does not equalize rates; a proportional-fair objective would need a nonlinear convex solver.
- **Runtime and scale.** Stage 1b needs 0.3–2.5 s per network, and exact MIS enumeration limited the study to 10 UAVs; larger networks would need column generation or a restricted MIS set.
- **Heuristic search.** Stage 1b searches discrete power levels and can stop in a local optimum.
- **Baselines.** MASPECT and learning-based allocators were not re-implemented.

8 Conclusion

The graph-based bandwidth allocation of [5] maximizes allocated bandwidth instead of data rate, and it allocates bandwidth under full-power interference. Restoring spectral efficiency in its objective yields an exactly solvable LP, letting a power-aware search choose the transmit powers before that LP more than doubles the achievable rate, and an alternating bandwidth–power stage then lowers power further while every QoS target stays met.

Over 200 paired trials per configuration, the combined scheme raised the data rate by 21–231% and EE by 6–95% in LoS conditions, and by up to 305% and 111% under mixed LoS/NLoS conditions, while every link kept the base scheme's worst-link rate to within 4% in LoS. For 3–5 UAVs it reached 87–96% of a near-optimal joint benchmark, against 34–46% for the base scheme. The price is a lower Jain fairness index and a runtime of up to 2.5 s for 10 UAVs. Future work will address proportional fairness, UAV mobility and scalable MIS generation.

Acknowledgements. Not applicable.

Declarations

- **Funding:** The authors did not receive support from any organization for the submitted work.
- **Competing interests:** The authors have no competing interests to declare that are relevant to the content of this article.
- **Ethics approval and consent to participate:** Not applicable.
- **Consent for publication:** Not applicable.
- **Data availability:** All raw and summarized simulation results are available in the repository listed under Code availability.
- **Code availability:** The simulation code and Google Colab notebook are available at https://github.com/srinivaskollimarlaece/GitHub_repository_files_v3.
- **Author contribution:** K. Srinivasa Rao: conceptualization, methodology, software, writing – original draft. S. Kannappan: supervision, writing – review and editing. G. Jyothi: investigation, visualization. All authors read and approved the final manuscript.

References

[1] Zeng, Y., Zhang, R., Lim, T.J.: Wireless communications with unmanned aerial vehicles:

Opportunities and challenges. IEEE Communications Magazine **54**(5), 36–42 (2016) https://doi.org/10.1109/MCOM.2016.7470933

[2] Mozaffari, M., Saad, W., Bennis, M., Nam, Y.-H., Debbah, M.: A tutorial on UAVs for wireless networks: Applications, challenges, and open problems. IEEE Communications Surveys & Tutorials **21**(3), 2334–2360 (2019)

[3] Mozaffari, M., Lin, X., Hayes, S.: Toward 6G with connected sky: UAVs and beyond. IEEE Communications Magazine **59**(12), 74–80 (2021)

[4] Jiang, X., Sheng, M., Zhao, N., Xing, C., Lu, W., Wang, X.: Green UAV communications for 6G: A survey. Chinese Journal of Aeronautics **35**(9), 19–34 (2022)

[5] Alnakhli, M.A., Mohamed, E.M., Fouda, M.M.: Bandwidth allocation and power control optimization for multi-UAVs enabled 6G network. IEEE Access **12**, 67405–67415 (2024) https://doi.org/10.1109/ACCESS.2024.3397165

[6] Anand, S., Sengupta, S., Chandramouli, R.: MAximum SPECTrum packing: A distributed opportunistic channel acquisition mechanism in dynamic spectrum access networks. IET Communications **6**(8), 872–882 (2012)

[7] Alnakhli, M., Anand, S., Chandramouli, R.: Joint spectrum and energy efficiency in device to device communication enabled wireless networks. IEEE Transactions on Cognitive Communications and Networking **3**(2), 217–225 (2017)

[8] Alnakhli, M.A., *et al.*: Joint optimization of spectrum and power control in 6G multi-UAV networks: Managing data redundancy. IEEE Access **13**, 132913–132925 (2025)

[9] Wu, Q., Zeng, Y., Zhang, R.: Joint trajectory and communication design for multi-UAV enabled wireless networks. IEEE Transactions on Wireless Communications **17**(3), 2109–2121 (2018)

[10] Fu, X., Ding, T., Peng, R., Liu, C., Cheriet, M.: Joint UAV channel modeling and power control for 5G IoT networks. EURASIP Journal on Wireless Communications and Networking **2021**(1), 106 (2021)

[11] Wang, X., Fei, Z., Huang, J., Zhang, J.A., Yuan, J.: Joint resource allocation and power control for radar interference mitigation in multi-UAV networks. Science China Information Sciences **64**(8), 182307 (2021)

[12] Lee, S., Lim, S., Chae, S.H., Jung, B.C., Park, C.Y., Lee, H.: Optimal frequency reuse and power control in multi-UAV wireless networks: Hierarchical multi-agent reinforcement learning perspective. IEEE Access **10**, 39555–39565 (2022)

[13] Zhang, Q., Wang, H., Feng, Z., Han, Z.: Many-to-many matching-theory-based dynamic bandwidth allocation for UAVs. IEEE Internet of Things Journal **8**(12), 9995–10009 (2021)

[14] Shah, A.F.M.S., Karabulut, M.A.: Optimization of drones communication by using metaheuristic optimization algorithms. Sigma Journal of Engineering and Natural Sciences **40**(1), 108–117 (2022) https://doi.org/10.14744/sigma.2022.00009

[15] Jain, K., Padhye, J., Padmanabhan, V.N., Qiu, L.: Impact of interference on multi-hop wireless network performance. Wireless Networks **11**(4), 471–487 (2005) https://doi.org/10.1007/s11276-005-1769-9

[16] Foschini, G.J., Miljanic, Z.: A simple distributed autonomous power control algorithm and its convergence. IEEE Transactions on Vehicular Technology **42**(4), 641–646 (1993)

[17] Yates, R.D.: A framework for uplink power control in cellular radio systems. IEEE Journal on Selected Areas in Communications **13**(7), 1341–1348 (1995)

[18] Luo, Z.-Q., Zhang, S.: Dynamic spectrum management: Complexity and duality. IEEE

Journal of Selected Topics in Signal Processing **2**(1), 57–73 (2008) https://doi.org/10.1109/JSTSP.2007.914876

[19] Tseng, P.: Convergence of a block coordinate descent method for nondifferentiable minimization. Journal of Optimization Theory and Applications **109**(3), 475–494 (2001) https://doi.org/10.1023/A:1017501703105

[20] Khuwaja, A.A., Chen, Y., Zhao, N., Alouini, M.-S., Dobbins, P.: A survey of channel modeling for UAV communications. IEEE Communications Surveys & Tutorials **20**(4), 2804–2821 (2018)

[21] Al-Hourani, A., Kandeepan, S., Lardner, S.: Optimal LAP altitude for maximum coverage. IEEE Wireless Communications Letters **3**(6), 569–572 (2014) https://doi.org/10.1109/LWC.2014.2342736

[22] Huangfu, Q., Hall, J.A.J.: Parallelizing the dual revised simplex method. Mathematical Programming Computation **10**(1), 119–142 (2018)

[23] Jain, R., Chiu, D.-M., Hawe, W.R.: A quantitative measure of fairness and discrimination for resource allocation in shared computer systems. Technical Report DEC-TR-301, Digital Equipment Corporation (1984)

[24] Wilcoxon, F.: Individual comparisons by ranking methods. Biometrics Bulletin **1**(6), 80–83 (1945)

[25] Holm, S.: A simple sequentially rejective multiple test procedure. Scandinavian Journal of Statistics **6**(2), 65–70 (1979)